Hand-feel soil texture observations to evaluate the accuracy of digital soil maps for local prediction of soil particle size distribution : A case study in Central France

RIicher-de-Forges, Anne C.; Arrouays, Dominique; Poggio, Laura; Chen, Songchao; Lacoste, Marine et al

PEDOSPHERE

www.elsevier.com/locate/pedosphere

Hand-feel soil texture observations to evaluate the accuracy of digital soil maps for local prediction of soil particle size distribution: A case study in Central France

CrossMark

Anne C. RICHER-de-FORGES[1,*], Dominique ARROUAYS[1], Laura POGGIO[2], Songchao CHEN[3], Marine LACOSTE[1], Budiman MINASNY[4,5], Zamir LIBOHOVA[6], Pierre ROUDIER[7], Vera L. MULDER[8], Hervé NÉDÉLEC[9], Guillaume MARTELET[10], Blandine LEMERCIER[11], Philippe LAGACHERIE[12] and Hocine BOURENNANE[1]

[1]*INRAE (Institut national de recherche pour l'agriculture, l'alimentation et l'environnement), Info&Sols Unit, Orléans 45075 (France)*
[2]*ISRIC (International Soil Reference and Information Centre) Wageningen, P.O. Box 353, Wageningen 6700 (The Netherlands)*
[3]*Zhejiang University-Hangzhou Global Scientific and Technological Innovation Center, Hangzhou 311200 (China)*
[4]*The University of Sydney, Sydney Institute of Agriculture. Eveleigh NSW 2015 (Australia)*
[5]*The University of Sydney, School of Life and Environmental Sciences, Eveleigh NSW 2015 (Australia)*
[6]*USDA-ARS (United States Department of Agriculture-Agricultural Research Service), Dale Bumpers Small Farms Research Center, 6883 S. State Hwy. 23, Booneville AR 72927 (USA)*
[7]*Landcare Research-Manaaki Whenua, Palmerston North 4442 (New Zealand)*
[8]*Soil Geography and Landscape Group, Wageningen University, P.O. Box 47, Wageningen 6700 (The Netherlands)*
[9]*Chambre d'Agriculture du Loiret, Orléans F-45000 (France)*
[10]*Bureau de Recherches Géologiques et Minières, BP 36009, Orléans cedex 2, Orléans 45060 (France)*
[11]*UMR SAS (Unité Mixte de Recherche "Sol Agro et hydrosystème Spatialisation") Institut Agro, INRAE, Rennes F-35000 (France)*
[12]*UMR LISAH (Unité Mixte de Recherche "Laboratoire d'Etude des Interactions entre Sol-Agrosystème-Hydrosystème"), INRAE, Institut Agro, IRD (Institut de Recherche pour le Développement), Montpellier F-34000 (France)*

ABSTRACT

Digital maps of soil properties are now widely available. End-users now can access several digital soil mapping (DSM) products of soil properties, produced using different models, calibration/training data, and covariates at various spatial scales from global to local. Therefore, there is an urgent need to provide easy-to-understand tools to communicate map uncertainty and help end-users assess the reliability of DSM products for use at local scales. In this study, we used a large amount of hand-feel soil texture (HFST) data to assess the performance of various published DSM products on the prediction of soil particle size distribution in Central France. We tested four DSM products for soil texture prediction developed at various scales (global, continental, national, and regional) by comparing their predictions with approximately 3 200 HFST observations realized on a 1:50 000 soil survey conducted after release of these DSM products. We used both visual comparisons and quantitative indicators to match the DSM predictions and HFST observations. The comparison between the low-cost HFST observations and DSM predictions clearly showed the applicability of various DSM products, with the prediction accuracy increasing from global to regional predictions. This simple evaluation can determine which products can be used at the local scale and if more accurate DSM products are required.

Key Words: digital soil mapping products, easy-to-understand tool, hand-feel observation, local use, map uncertainty, prediction performance, spatial extent, visual assessment

INTRODUCTION

Digital soil mapping (DSM) (McBratney *et al.*, 2003) has moved from the research stage to the operational stage (Minasny and McBratney, 2016; Arrouays *et al.*, 2017a; Zhang *et al.*, 2017; Arrouays *et al.*, 2020). Consequently, gridded maps of soil properties are freely available online. However, this swift development has provided end-users with several DSM products generated using different models, calibration/training data, and covariates at spatial scales, varying from global to local (Padarian *et al.*, 2020; Chen *et al.*, 2022). Users of DSM products include soil scientists, agronomists, climate change modelers, biodiversity conservation specialists, economists, hydrologists, land-use planners, governments, and policymakers. Stakeholders, such as farmers or forest managers, are also interested in

using DSM products for their farms, but they require fine-resolution soil information that can assist land management decisions.

Most of the predicted performances of DSM products have been evaluated using various cross-validation methods (Liu *et al*., 2020; Chen *et al*., 2022) or independent probability sampling, as recommended by Brus *et al*. (2011) and Helfenstein *et al*. (2022). Although many DSM products now provide estimates of uncertainties using various methods (Chen *et al*., 2022), these uncertainties remain largely ignored by end-users (Richer-de-Forges *et al*., 2019; Arrouays *et al*., 2020). Therefore, there is an urgent need to provide easy-to-understand tools to communicate map uncertainty and help end-users assess the reliability of using DSM products at local scales.

Some studies have compared DSM products with existing soil maps (Bazaglia Filho *et al*., 2013; Bishop *et al*., 2015; Ellili-Bargaoui *et al*., 2020; Rossiter *et al*., 2021) and/or point measurements (Ungaro *et al*., 2010; Tifafi *et al*., 2018; Ellili-Bargaoui *et al*., 2019, 2020). However, few studies have used soil survey information acquired during soil mapping campaigns as input to DSM models or to evaluate DSM products. This soil information can be obtained from legacy or recent survey data. Extensive information is obtained during surveys (*e.g*., soil colour, hand-feel soil texture, and reaction to hydrogen chloride), which could be useful for the rapid assessment of DSM prediction performance.

Soil texture (ST), the relative proportions of sand, silt, and clay, is one of the most frequently determined soil properties. It can be assessed in the laboratory or estimated manually by soil surveyors in the field (NSSC-NRCS-USDA, 2012). The main differences between hand-feel ST (HFST) and laboratory-measured ST (LAST) were summarized by Salley *et al*. (2018). Briefly, HFST is estimated *via* sensory tests between the fingers and thumb of a sample taken from a horizon (or a fixed depth layer) to allocate the soil sample to an ST class. Laboratory-measured ST is characterized by the contents of clay, silt, and sand using a standardized method of physical separation based on size and density after pre-treatments (*e.g*., removal of organic matter). Both results can be plotted in the soil "texture triangle", which can differ between and even within countries (Richer-de-Forges *et al*., 2008a).

Compared with LAST, HFST is conditional on uncertainty and subjectivity. However, in conventional soil surveys, legacy observations of HFST outnumber those of LAST (Richer-de-Forges *et al*., 2022). Furthermore, when evaluated by experienced soil surveyors, HFST often correlates well with LAST (Vos *et al*., 2016; Salley *et al*., 2018; Malone and Searle, 2021). A previous study conducted in Central France (Richer-de-Forges *et al*., 2022) showed that well-trained and professional soil surveyors could predict ST classes with much higher accuracy (overall accuracy: 73%) than that previously reported in the literature (Vos *et al*., 2016; Salley *et al*., 2018; Malone and Searle, 2021). This result was attributed to experienced surveyors who knew the pedogenic context of their studied area well and conducted collaborative fieldwork with neighbouring regions.

Rossiter *et al*. (2015) posited that "An obvious check is how well new observations fit an existing soil-landscape model used for DSM". However, for local applications, only a small amount of quantitative data are available, which limits the assessment of the accuracy of DSM predictions. Thus, in the present study, we attempted to use a large amount of HFST data to assess the performance of published DSM products in the prediction of soil particle size distribution at a local scale.

In the present study, we used the HFST observed during soil survey campaigns to produce a new semi-detailed map at a 1:50 000 scale (over *ca*. 55 000 ha) in Central France (the same region as Richer-de-Forges *et al*. (2022)). We evaluated the accuracy of several DSM products that were obtained at several geographical extents: global, continental (Europe Union (EU)), national (France), and French department (*ca*., 6 000 km^2), using various covariates. Aiming to develop an easy-to-understand indicator of the local performances of various DSM predictions based on the differences between LAST predictions and HFST observations, the present study capitalized on a large amount of HFST data, which are cheap and easy to measure. The proposed method can be used as a general scheme for evaluating the applicability of DSM products.

MATERIALS AND METHODS

Study area

The study area (Fig. S1, see Supplementary Material for Fig. S1) covers the 1:50 000 soil map of Pithiviers in the Loiret Department, France, produced by Nédélec (2015) using conventional soil mapping. This map and associated soil point data were neither used to develop the global, national, or regional DSM products, nor used to create the conventional 1:250 000 soil map of the Loiret Department (Richer-de-Forges *et al*., 2008b).

The Loiret Department is located in Central France as one of the flattest departments in France, with an altitude ranging from 70 m above sea level (asl) in the northeast to 270 m asl in the southeast (Richer-de-Forges *et al*., 2008b). It has a continental-oceanic climate with a mean annual temperature of 11.5 °C and a mean annual rainfall of 700 mm. The Loire River crosses this department from southeast to southwest. In the north of Loiret, soils belong to the agricultural Beauce region and are mainly developed from periglacial loess deposits that cover limestone bedrocks. In the south

of the Beauce region and from north to south, the main soils encountered are Vertisols developed on marl, followed by Arenosols, Planosols, luvic Cambisols, and Cambisols developed on complex ancient deltaic deposits, which are mainly composed of clay and sand. The Loire Valley crosses these deposits, where sandy Fluvisols are developed, and the surrounding quaternary ancient terraces, on which various luvic Cambisols are found, more or less differentiated depending on their age (Richer-de-Forges *et al.*, 2008b). Pithiviers is located in the north of the Loiret Department (Fig. 1) and mainly includes Cambisols (except for dystric Cambisols) developed on periglacial loess deposits on limestone, Vertisols developed on marl, and various soils developed on complex sandy and clayey deltaic deposits in the extreme southwestern part (Nédélec, 2015).

a

Arenosols
Dystric Cambisols
Eutric Cambisols
Colluvic Regosols
Haplic Planosals
Stagnosols
Gleysols
Vertisols
Calcaric Cambisols
Luvic Cambisols

Calcaric Cambisols-Stagnosols
Anthroposols/Technosols
Cambisols-Stagnosols
Colluvics Regasols-Stagnosols
Luvic Cambisols-Stagnosols
Hypereutric Cambisols
Hypereutric Cambisols-Stagnosols
Epileptic hypereutric Cambisol
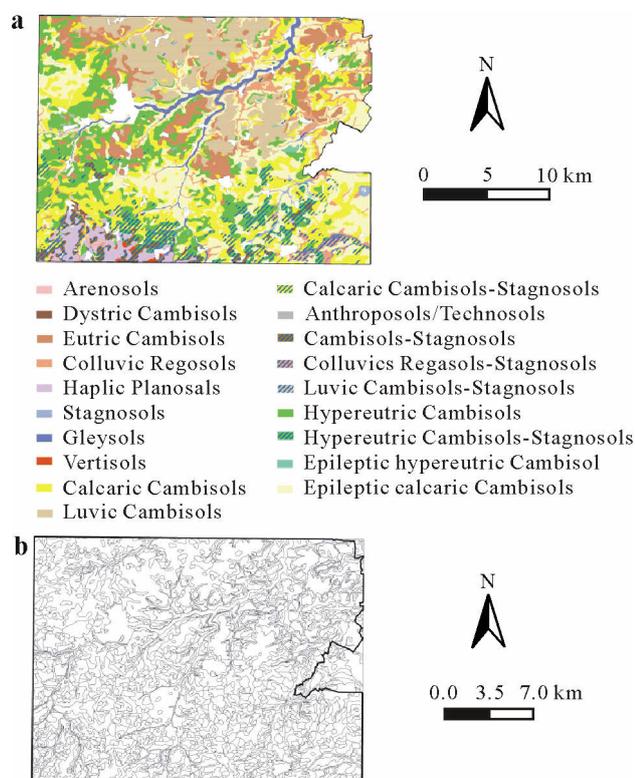Epileptic calcaric Cambisols

b

Fig. 1   Conventional soil map (1:50 000) of Pithiviers, France, showing dominant soil types per polygon (a) and the original polygons of this soil map (b).

Using HFST data to evaluate the accuracy of the Pithiviers soil map

We selected 3 263 HFST soil observation points on the Pithiviers map with HFST estimates using the Aisne texture triangle (Jamagne, 1967) at two depths: 0–30 and 30–60 cm (Fig. 2). For the HFST at 0–30 cm, we selected the HFST of the upper horizon (excluding the O horizon). Most soils were cultivated; therefore, they corresponded to the plough layer. For forest and very rare grassland soils, we selected
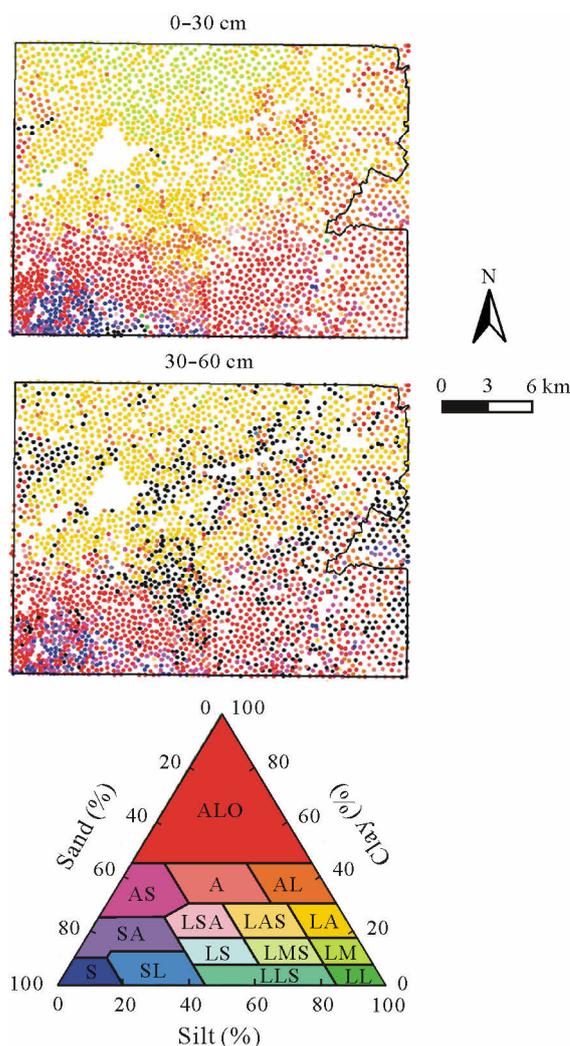
Fig. 2   Hand-feel soil texture of 3 263 soil points in Pithiviers, France estimated using the Aisne texture triangle. ALO = heavy clay; A = clay; AL = silty clay; AS = sandy clay; LA = clayey silt; LAS = sandy clayey silt; LSA = clayey sand silt; SA = clayey sand; S = sand; SL = silty sand; LL = silt; LS = sandy silt; LMS = sandy medium silt; LM = medium silt; LLS = sandy medium silt. Points in black indicate no data.

the dominant HFST values observed at 0–30 cm (excluding O horizon).

Broad-scale DSM predictions

Three broad-scale DSM products of ST prediction covering the soil map of the Pithiviers area were selected. They included the global product SoilGrids 2.0 map (Poggio *et al.*, 2021), the EU map developed by Ballabio *et al.* (2016) that utilizes the land use and coverage area frame survey (LUCAS-Soil) topsoil data (LUCAS-Soil map), and the GlobalSoilMap product for France (GlobalSoilMap-France) (Mulder *et al.*, 2016). Their primary characteristics are described as follows.

SoilGrids 2.0 map.   SoilGrids 2.0 map is a global digital soil map developed using a tri-dimensional machine

learning method that predicts the spatial distribution of several soil properties at various depths, as defined by the GlobalSoilMap specifications (Poggio *et al.*, 2021). We used clay, silt, and sand content maps at depths of 5–15 and 30–60 cm. As most of the region is intensively cultivated and ploughed, we hypothesized that the ST at 5–15 and 0–30 cm would be similar. However, this may not always be true, as in the case of forested areas. The grid spacing was 250 m.

LUCAS-Soil map. The LUCAS-Soil included the main properties of topsoil (0–20 cm) in 23 member states of EU (Orgiazzi *et al.*, 2018). Ballabio *et al.* (2016) used LUCAS-Soil data to predict DSM of particle size distribution (*i.e.*, clay, silt, and sand contents) over Europe based on a grid spacing of 500 m.

GlobalSoilMap-France. The methodology of GlobalSoilMap-France product has been detailed by Mulder *et al.* (2016). Digital maps were created following the GlobalSoilMap specifications using point observations from legacy data of France (Arrouays *et al.*, 2014a, b). Grid spacing was 90 m.

Regional-scale DSM product

We built a regional DSM model only using soil LAST data of 988 soil profiles in Loiret to predict clay, sand, and silt contents. Particle size distribution was measured according to the French standard, the pipette method (Afnor Editions, 2003). The map was generated using the quantile regression forest (QRF) model in the R package "quantregForest" (Meinshausen, 2006) with the covariates listed in Table I. The performance of the model was evaluated using a 10-fold cross-validation procedure. Grid spacing was 25 m (Table I).

However, the maps were incomplete in certain areas owing to missing values of some covariates, particularly in built-up areas. These covariates were those obtained by airborne gamma-rays (U, K, Th, and total count; Table I). They were not available in cities and small military airports because the aircraft was not allowed to fly at a very low elevation and/or to take images over these areas. To overcome this limitation, missing data were filled in by modelling using the ranger package (Wright and Ziegler, 2017) and other covariates. We randomly selected 10 000 samples from the map to build a model and systematically filled in the missing values. Mulder *et al.* (2016) could not use this method in France because the spatial coverage of the entire territory was incomplete.

Comparison between modelled LAST predictions and observed HFST classes

Plotting LAST prediction against each observed HFST class. For each observed HFST class, we plotted the corresponding DSM prediction of clay, silt, and sand contents in the texture triangle. For each HFST class, we calculated the density of predicted LAST points in the triangle using the function "kde2d: Two-Dimensional Kernel Density

TABLE I

Environmental covariates used to generate the map using the quantile regression forest model in the R package quantregForest

Covariate	Definition (unit)	Resolution/spacing	Reference
		m	
DEM[a]	Elevation (m)	25 × 25	IGN, 2011
DEM derivative			
Dppr	Hydrological distance from each pixel to its nearest outlet (m)	250 × 250	IGN, 2011
Beven index	Beven index (m)	25 × 25	IGN, 2011
Courb_mixte	Mixed curvature (m)	25 × 25	IGN, 2011
Curv_long	Profile curvature (m)	25 × 25	IGN, 2011
Curv_plan	Plan curvature (m)	25 × 25	IGN, 2011
Slope	Slope (°)	25 × 25	IGN, 2011
Aspect	Aspect (°)	25 × 25	IGN, 2011
Lithology (17 classes)	Parent material	1/250 000	Richer de Forges *et al.*, 2008b
Land cover (20 classes)	Landscape Sentinel-2 2018	10 × 10	Thieron *et al.*, 2022
Gamma-ray data			
U	Uranium (gamma) (mg kg^{-1})	200 × 200	Martelet *et al.*, 2014
K	Potassium (gamma) (× 10 g kg^{-1})	200 × 200	Martelet *et al.*, 2014
Th	Thorium (gamma) (mg kg^{-1})	200 × 200	Martelet *et al.*, 2014
Tot	Total gamma-ray (nGy^{-1} h)	200 × 200	Martelet *et al.*, 2014
GlobalSoilMap-France			
Silt_l0	Mean silt content at 5–15 cm (g kg^{-1})	90 × 90	Mulder *et al.*, 2016
Silt_l30	Mean silt content at 30–60 cm (g kg^{-1})	90 × 90	Mulder *et al.*, 2016
Sand_l0	Mean sand content at 5–15 cm (g kg^{-1})	90 × 90	Mulder *et al.*, 2016
Sand_l30	Mean sand content at 30–60 cm (g kg^{-1})	90 × 90	Mulder *et al.*, 2016
Clay_l0	Mean clay content at 5–15 cm (g kg^{-1})	90 × 90	Mulder *et al.*, 2016
Clay_l30	Mean clay content at 30–60 cm (g kg^{-1})	90 × 90	Mulder *et al.*, 2016

[a] DEM = digital elevation model.

Estimation" of the R package "soiltexture" (Moeys *et al*., 2018) (version 1.5.1). This allowed a visual evaluation of the distribution of each LAST prediction for each corresponding observed HFST class in the texture triangle.

Calculation of the shortest distance between predicted LAST and observed HFST. To assess the accuracy of the DSM prediction of clay, silt, and sand contents, we calculated the shortest distance from the predicted LAST to the limits of the observed HFST class using the R packages "soiltexture" (Moeys *et al*., 2018) and "rgeos" (Bivand *et al*., 2021). If the predicted LAST was consistent with the observed HFST, the distance was equal to 0. We then calculated the mean value of this distance for each HFST class and used it as an indicator of the consistency between the observed HFST and predicted LAST values. We normalized the distance by transforming its maximal value to 1 and its minimum value to 0. This normalized distance had no units.

RESULTS

Visual comparison of the various DSM products

Four DSM products of clay, silt, and sand contents in Pithiviers were obtained at the global, continental, national, and regional levels. In the following subsections, we briefly described each map and then provided a comparison of the patterns observed in these maps.

SoilGrids 2.0. map. Figure 3 shows the spatial distribution of mean clay, silt, and sand contents predicted

by SoilGrids 2.0 (Poggio *et al*., 2021). Overall, this spatial distribution was characterized by a relatively large homogeneous area. The spatial distribution patterns of the topsoil (5–15 cm) and subsoil (30–60 cm) were also similar.

LUCAS-Soil map. Figure 4 shows the spatial distribution of mean clay, silt, and sand contents from a European DSM product calibrated using the LUCAS-Soil data (Ballabio *et al*., 2016). The predicted values were more variable than those of the SoilGrids2.0 map. However, there were some prominent spatial patterns, such as the sandy area in the southwestern part of the map and rather large valleys in the northern part of the silt and sand maps.

GlobalSoilMap-France. The distribution by GlobalSoilMap-France (Mulder *et al*., 2016) showed a largely uniform pattern (Fig. 5). The sand maps were relatively similar to those predicted by SoilGrids 2.0.

Regional maps. Figures 6, 7, and 8 show the spatial distribution of median clay, silt, and sand contents generated using the regional model, together with their lower and upper prediction intervals (5% and 95% percentiles). The silt maps (Fig. 7) showed the most contrasting patterns in the north-eastern part. The valleys were clearly visible on most of the maps, and the sandiest area in the southwest was more clearly delineated.

Comparison between maps. There were similarities and discrepancies between the four DSM products. All maps clearly showed a siltier zone in the northwestern region, especially in the topsoil. The GlobalSoilMap-France exhibited
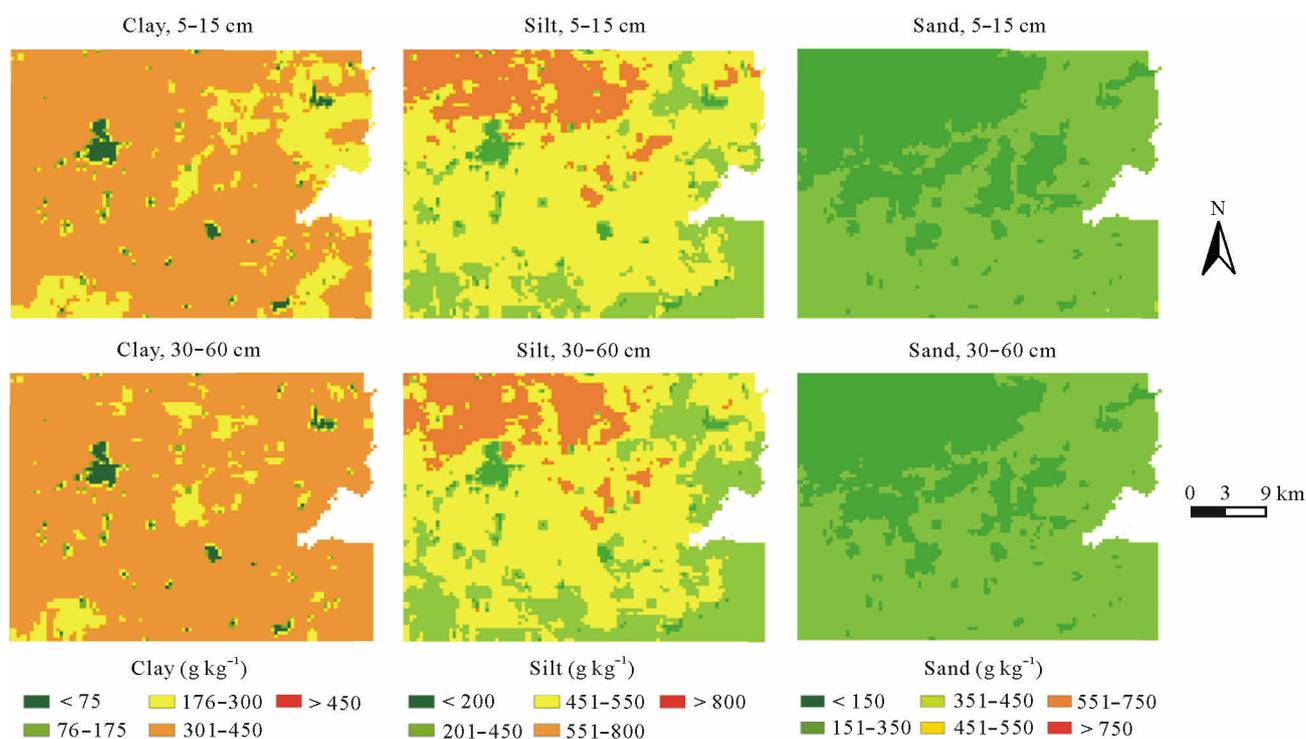

Fig. 3   Spatial distribution of soil particle size classes in Pithiviers, France, extracted using the SoilGrids model.
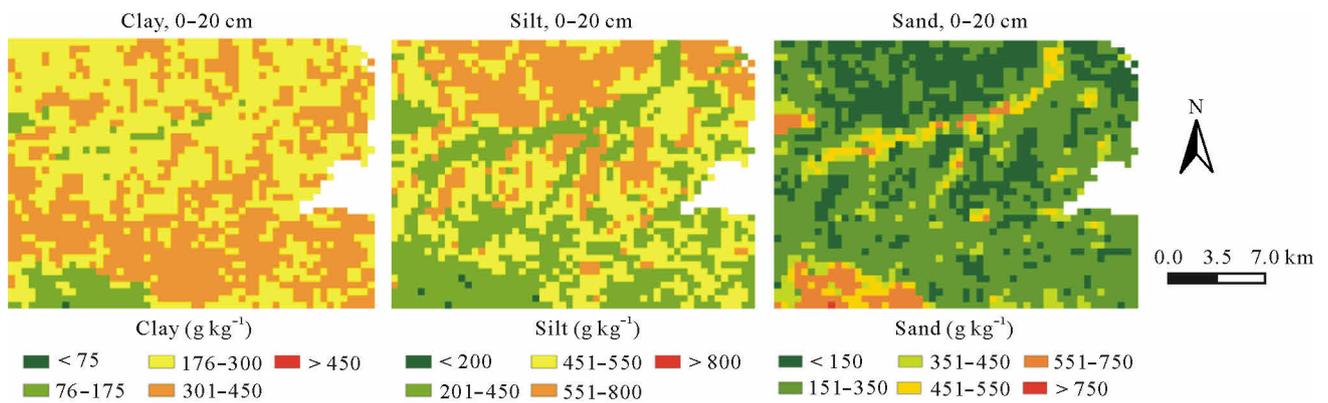
Fig. 4   Spatial distribution of soil particle size classes in Pithiviers, France, extracted using the LUCAS-Soil model.
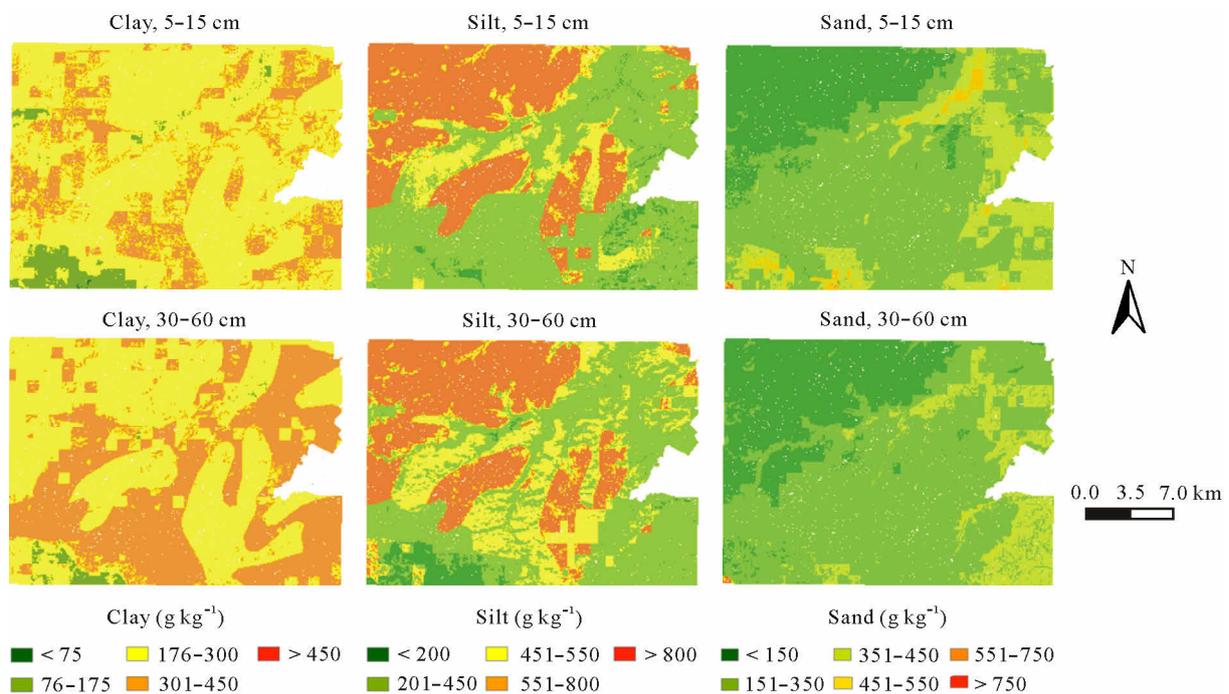

Fig. 5   Spatial distribution of soil particle size classes in Pithiviers, France, extracted using the GlobalSoilMap for France model.

some large polygons with sharp boundaries because of the 1:1 000 000 soil parent material map used as a covariate and some artifacts (large square patterns) due to coarse climate data, as pointed out by Mulder *et al.* (2016). A more sandy area was predicted using the SoilGrids 2.0, GlobalSoilMap-France, and regional model than the LUCAS-Soil data in the extreme southwestern part of the map, mainly for subsoils. This sandy area was also predicted using LUCAS-Soil for the topsoil and using regional model for both depths. Patterns linked to rivers were not well identified by SoilGrids 2.0, although some were clearly evidenced in the regional model. The prediction intervals were quite large (Figs. 6 and 7). The maps of the regional model corresponded to a finer resolution (25 m × 25 m). As the regional model used GlobalSoilMap-France as covariates, some of the regional maps exhibited

artifacts. The gamma-ray and digital elevation model (DEM) derivative covariates resulted in finer map details.

Density of LAST DSM predictions for each observed HFST class

We present the LAST DSM predictions for each HFST class observed from the soil survey data for the 1:50 000 map.

Topsoil.   Figure S2 (see Supplementary Material for Fig. S2), from left to right, shows how the LAST values predicted by each model distributed on each observed HFST class. All the predictions tended to underestimate the clay content for the HFST heavy clay (ALO) class, even in the regional model. SoilGrids showed a very compact cluster on the left side of the silty clay (AL) class. The LAST AL class was better predicted by the regional, LUCAS-Soil,
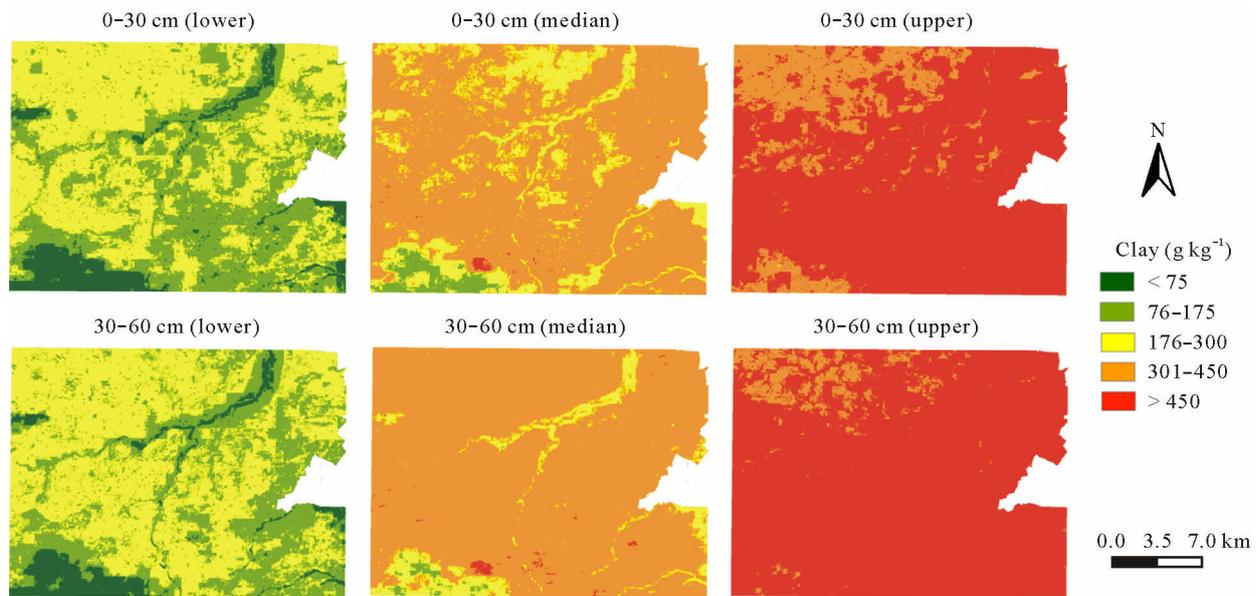
Fig. 6   Spatial distribution of particle size classes for soil clay in Pithiviers, France, extracted using the regional model. Lower and upper maps correspond to the 5% and 95% percentiles, respectively.
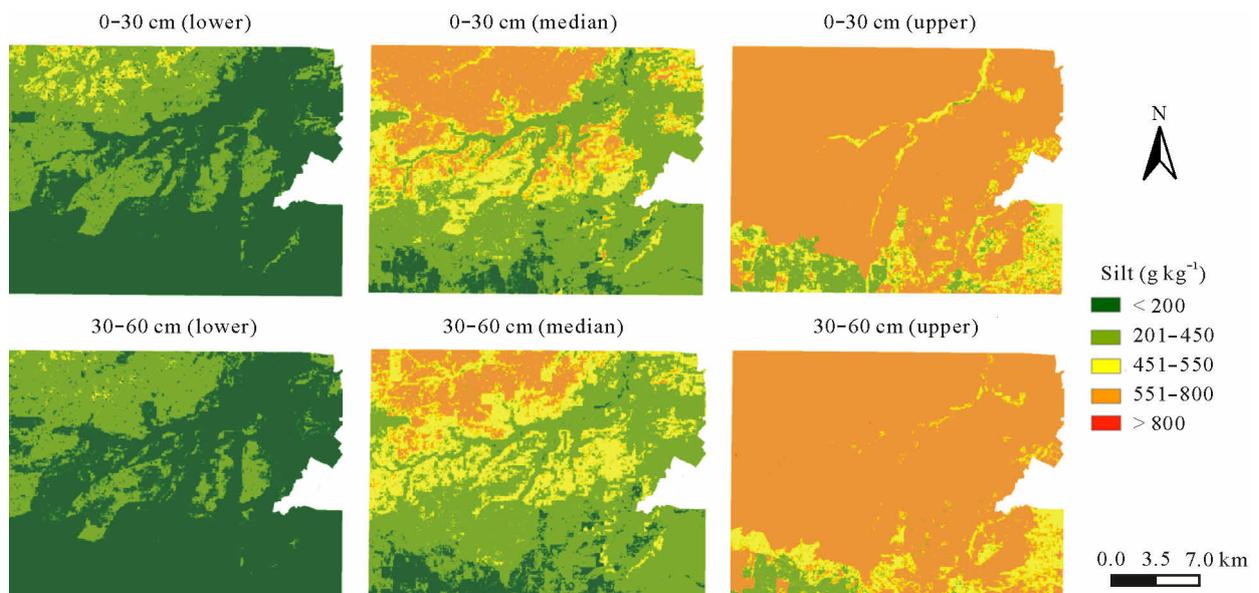
Fig. 7   Spatial distribution of particle size classes for soil silt in Pithiviers, France, extracted using the regional model. Lower and upper maps correspond to the 5% and 95% percentiles, respectively.

and SoilGrids models. For the clay (A) class, the regional model gave a good prediction, whereas the predictions of GlobalSoilMap-France and LUCAS-Soil were scattered, and SoilGrids identified A as AL. The LAST sandy clay (AS) class was not well predicted by the models, and their predictions worsened with the increasing geographical extent of the model. The clayey silt (LA) class was not well predicted but the predictions of all four models were consistent and were mainly located in adjacent classes, especially in AL. In this study area, the texture of the topsoil was mostly LA and AL; therefore, the discrepancy between classes

does not necessarily imply a large difference in LAST. For the sandy clayey silt (LAS) class, the predictions of GlobalSoilMap-France were the best, whereas the clayey sand silt (LSA) class showed considerable dispersion in the regional model and was more clustered in other models. The regional model predicted the sandy clay (SA) class quite well, but this class was poorly predicted by GlobalSoilMap-France and LUCAS-Soil and was completely missed by SoilGrids. The sand (S) class was underestimated by all the models (especially by SoilGrids), whereas the three remaining HFST classes (medium silt, sandy silt, and sandy

Fig. 8 Spatial distribution of particle size classes for soil sand in Pithiviers, France, extracted using the regional model. Lower and upper maps correspond to the 5% and 95% percentiles, respectively.
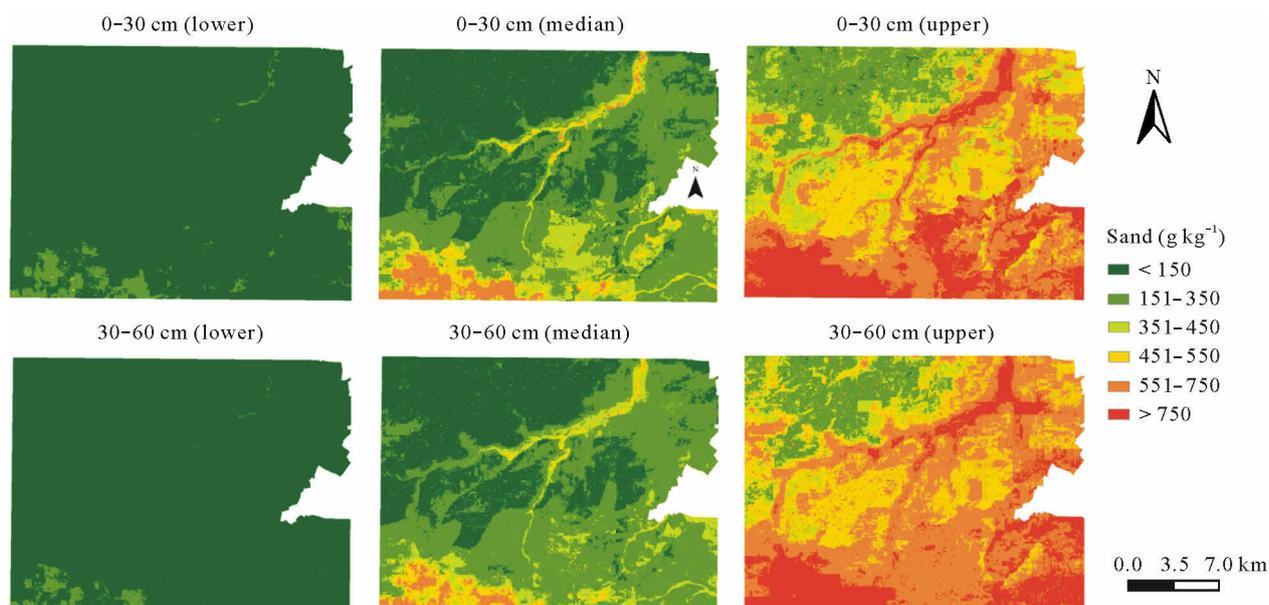
medium silt) were not predicted by any of the models. Figure S2 revealed that SoilGrids had a strong tendency to predict very compact or similar LAST values for all HFST classes, most of them within or adjacent to the AL class. In general, the regional model performed slightly better than the GlobalSoilMap and LUCAS-Soil models; however, this was not the case for all HFST. In all cases, the extreme values at the corners of the triangle tended to be underestimated, particularly in SoilGrids. In general, the regional model performed better than the other models, whereas GlobalSoilMap-France and LUCAS-Soil map gave a rather similar distribution for topsoil.

Subsoil. For the subsoil (Fig. S3, see Supplementary Material for Fig. S3), the LUCAS-Soil DSM product had no data; however, for the other models, the results were consistent with those obtained for the topsoil. The tendency for SoilGrids to overestimate the AL class was also evident here, whereas predictions were generally better for the regional model than for GlobalSoilMap-France, with noticeable exceptions for HFST LA and LAS.

Distance between predicted LAST and observed HFST

To calculate the accuracy of the DSM product predictions for each ST class by comparing with soil survey HFST observations, we calculated the normalized distance between the predicted points and the closest boundary of their corresponding HFST (Fig. S4, see Supplementary Material for Fig. S4).

In general, the regional model predictions were the closest to HFST classes (mean distance = 0.21 for topsoil and 0.27 for subsoil), followed by GlobalSoilMap predictions

(mean distance = 0.28 for topsoil and 0.32 for subsoil). The LUCAS-Soil (mean distance = 0.24 for topsoil) and SoilGrids (mean distance = 0.32 for topsoil and 0.36 for subsoil) presented the farthest distances.

Most models did not predict the extreme sandy and silty classes well. This situation was worse for SoilGrids, particularly for sandy HFST. Nevertheless, SoilGrids performed well for the HFST adjacent to AL. However, SoilGrids mostly predicted ST in the area as AL and nearby ST classes (Figs. S2 and S3). The LUCAS-Soil model performed well for the central values of the HFST classes.

DISCUSSION

Limitations of the study

Can we draw conclusions from a local example? This study was limited to an area located in Central France (518.4 km^2). Therefore, the results may not be generic, and the conclusions may not be valid for other parts of the world. Nevertheless, our results are consistent with the existing evaluations of local or national DSM products (Bishop *et al.*, 2015; Guevara *et al.*, 2018; Vitharana *et al.*, 2019; Ellili-Bargaoui *et al.*, 2020; Roudier *et al.*, 2020). In general, maps built from broader data perform worse on local predictions (Caubet *et al.*, 2019; Chen *et al.*, 2020). This is not surprising as broader models generally capture large trends on the scale they are produced. This is logical if the following points are considered: the relative importance of the controlling factors of soil properties differ according to the scale at which they are studied, the density of the training points (soil observations) is often lower when geographical coverage

increases, and the nature and resolution of covariates also depend on the scale at which they are used. In this study the number of soil profiles available to generate SoilGrids products in France was limited. The observations of LUCAS-Soil were also less dense than those of the GlobalSoilMap and were limited to the topsoil. The GlobalSoilMap-France (Mulder *et al*., 2016) did not capture all soil variability in France. The regional model performed better than the national product (GlobalSoilMap-France), as it included new data that became available but the latter was produced in 2014. This point advocates a regular update of DSM products when new data become available (Arrouays *et al*., 2017a, b). Note that this possibility has been frequently maintained as an advantage of DSM compared to traditional soil mapping (McBratney *et al*., 2003; Arrouays *et al*., 2020). Although mentioned in several papers (Hengl *et al*., 2014; Mulder *et al*., 2016; Arrouays *et al*., 2017a), the automated updating of such products is still not operational. As computational power increases (Padarian *et al*., 2019, 2020), incorporating new covariates and building new models as new data become available through a well-documented code, and the procedure should be straightforward. Therefore, automated updating of DSM predictions should become a standard practice in the near future. The proposed method is influenced by the relative areas of the ST classes in the triangle. Thus, it is difficult to hypothesize how this method could be performed with triangles having a different number of ST classes. According to Richer-de-Forges *et al*. (2022), most triangles used worldwide have 12–18 classes, but the range is from 3 to 47 classes. A map with a few large classes may appear more accurate than that with many classes mostly because of the simpler legend. Therefore, we should keep in mind that the areas covered by classes (and thus the range of particle size values) differ among triangles. In other words, a ST class with a large area would lead to a higher probability of a DSM prediction to be allocated to that class and could create a false impression of high accuracy, *e.g*., the ALO (heavy clay) class can have a clay content between 50% and 80%. Nevertheless, because DSM products predict sand, silt, and clay contents (not ST classes), anomalous predictions, such as those observed for SoilGrids in which very large areas are predicted as AL, would be visible. Therefore, the proposed method can be used as a general scheme for evaluating the applicability of DSM products. In contrast, the calculation and illustration of distance between predicted points and HFST will be more affected by the ST class area, *i.e*., the larger the ST class area, the shorter the distance to the limit of the class.

Is our example a worst-case scenario?　As described in the previous section, the training data used for global modelling (SoilGrids and LUCAS-Soil) were sparse and/or restricted to topsoil. Another important point is that Loiret

is the flattest department in France. Therefore, it seems logical that coarse-resolution DEMs, such as those used for global modelling, are not effective in capturing local soil variability. In addition, a regional model was developed using detailed covariates that were not available for larger areas (detailed DEM and airborne gamma-ray data). These detailed covariates proved very efficient in other parts of France (Lacoste *et al*., 2011; Martelet *et al*., 2013; Loiseau *et al*., 2020) and many other parts of the world (Megumi and Mamuro, 1977; Wilford, 2012; Dierke and Werban, 2013; Gray *et al*., 2016; Padarian *et al*., 2019). Evidently, some soil processes and controlling factors occur at more detailed scales than those captured by global models using coarse-resolution covariates. Hence, the global models were unable to capture the north-western plateaus with the siltiest topsoil texture. The regional model underestimated the silt content and overestimated the clay content of the topsoil of these plateaus. This is likely because the number of training points in the plateaus was rather small. However, the spatial pattern of the map allowed us to delineate this specific soilscape with greater accuracy. This is consistent with the results of Chen *et al*. (2021), who showed that using fine resolution covariates, the thickness of loess (TOL) over the calcareous area was larger in the northern flat plateaus, and soils with large TOL are prone to illuviation resulting in lower clay content and siltier topsoil. Overall, these results advocate using more relevant and detailed covariates for regional or local DSM when available and ensuring the data cover the whole soilscape.

Inconsistency between covariates and data support.　A general issue in evaluating DSM prediction performance is that in many cases, the training and evaluation data are point measurements, whereas the covariates are areal data. Defining an "optimal" grid size is still being discussed (Bishop *et al*., 2015; Biggs *et al*., 2021; Szatmári *et al*., 2021) to deliver DSM products using more relevant spatial supports (farms, soil mapping units, watersheds, administrative units, *etc*.) and convey their uncertainties to decision makers (Heuvelink and Pebesma, 1999; Vaysse *et al*., 2017). In the present study, we evaluated the prediction performance using point data. Further research should use other supports for this evaluation. However, we should stress that our objective was to assess if the predictions were useful at the local scale, and therefore a too large spatial support could be impractical for use in soil management.

HFST has more uncertainty than LAST.　We used HFST data to evaluate the performance of the LAST predictions. We made the overwhelming assumption that HFST observations were the true values. However, this was not the case. Although for the same ST class, HFST may lead to different results when compared to the LAST projected (Foss *et al*., 1975; Hodgson *et al*., 1976; Akamigbo, 1984; Post

et al., 1986; David, 1999; Carlile *et al.*, 2001; Minasny and McBratney, 2001; Franzmeier and Owens, 2008; Vos *et al.*, 2016; Salley *et al.*, 2018; Malone and Searle, 2021), this was not the case for most observations. In the French Central region, Richer-de-Forges *et al.* (2022) showed that the overall accuracy of LAST predictions using HFST was 73%. This was even larger when adjacent ST classes were considered. Even if HFST carries an inherent uncertainty, the present results showed that HFST was increasingly consistent with DSM LAST predicted values when the models were less global and used more local covariates.

Practical application of this study

Using field HFST observations as data to evaluate the prediction performances of various DSM LAST predictions may help to provide a first assessment of the goodness of these predictions. When the training area is large and covariate resolution is high, predictions tend to be smooth. Such a quick check may help end-users decide which product to use or if a soil map is adequate. For DSM practitioners, this method can reveal whether a map is uncertain and requires a higher training point density or new detailed covariates. This study also advocates storing raw HFST values in soil databases and recording both HFST and LAST values, even when they are available at the same locations. The HFST data can be used to check whether DSM products are adequate or over-smoothing ST variability, considering the scale at which end-users intend to use these data.

Nevertheless, we caution against incorporating uncertain HFST values that may come from citizen science (Rossiter *et al.*, 2015; Salley *et al.*, 2018; Head *et al.*, 2020). We must stress that very experienced soil surveyors collected the HFST data used in the present study. Salley *et al.* (2018) demonstrated that training was important for HFST allocation.

Our results do not imply that global predictions are unusable but caution their use on a local scale. Moreover, the results advocate the need for local DSM at a finer scale and using more relevant and finer-resolution covariates depending on the local pedological context. This may involve having a more precise DEM at different spatial and vertical resolutions, using some relevant covariates that are not available at the global scale (*e.g.*, accurate lithological maps, airborne gamma-ray data, high-resolution remote sensing data, and vegetation maps) (Lagacherie *et al.*, 2012; Poggio *et al.*, 2013; Loiseau *et al.*, 2020; Heitkamp *et al.*, 2021), exploring spatial disaggregation for broader scale maps, or incorporating local pedological knowledge (Nauman and Thompson, 2014; Odgers *et al.*, 2014a, b; Holmes *et al.*, 2015; Machado *et al.*, 2018; Vincent *et al.*, 2018; Ellili-Bargaoui *et al.*, 2019, 2020; Ma *et al.*, 2019; Møller *et al.*, 2019). Our results also support the future strategy of DSM

in France, *i.e.*, to produce more local DSM maps at the local scale, as recommended by Voltz *et al.* (2020). A future study will explore whether spatially dense HFST data could be used to produce digital LAST maps and/or to improve existing DSM products.

CONCLUSIONS

Predicting particle size distribution is a common objective of DSM, as texture influences many soil processes. However, the relevance of using global or continental DSM products for local use is questionable. Conducting independent validation at a local scale implies the high cost of laboratory measurements. Here, we proposed a cheap and straightforward assessment of the performance of predictions by using HFST over an area that was underrepresented in global, continental, national, and regional DSM predictions. The comparison between the low-cost observed HFST and DSM predictions clearly showed the applicability of various DSM products, with prediction performance decreasing from global to regional predictions. This simple evaluation can determine which products can be used at a local scale and if more accurate DSM products are required. The visual interpretation of the predicted maps and the scattering of the predicted ST on a texture triangle for each observed HFST class may help to determine whether a DSM product is locally usable. It can also help to identify areas with a higher density of LAST measurements and/or if more relevant covariates are necessary. The example presented in this study stresses that some global and continental DSM products may not be sufficiently accurate for local use. A higher training point density and more precise and relevant covariates for local soilscapes are required to produce an accurate local DSM.

by the Région Centre-Val de Loire BRGM, and the "Fonds européen de développement regional" European funds. This study was conducted under the framework of CES CNS Théia for DSM. The authors thank Dr. David Rossiter and the two anonymous reviewers who provided helpful comments for improving this article.

SUPPLEMENTARY MATERIAL

Supplementary material for this article can be found in the online version.

REFERENCES

Afnor Editions. 2003. Qualité du sol—Détermination de la distribution granulométrique des particules du sol—Méthode à la pipette. NF X31-107. Available online at https://www.boutique.afnor.org/norme/nf-x31-107/qualite-du-sol-determination-de-la-distribution-granulometrique-des-particules-du-sol-methode-a-la-pipette/article/721991/fa124875 (verified on July 18, 2023).

Akamigbo F O R. 1984. The accuracy of field textures in a humid tropical environment. *Soil Surv Land Eval.* **4**: 63–70.

Arrouays D, Grundy M G, Hartemink A E, Hempel J W, Heuvelink G B M, Hong S Y, Lagacherie P, Lelyk G, McBratney A B, McKenzie N J, Mendonca-Santos M D L, Minasny B, Montanarella L, Odeh I O A, Sanchez P A, Thompson J A, Zhang G L. 2014a. GlobalSoilMap: Toward a fine-resolution global grid of soil properties. *Adv Agron.* **125**: 93–134.

Arrouays D, Lagacherie P, Hartemink A E. 2017a. Digital soil mapping across the globe. *Geoderma Regional.* **9**: 1–4.

Arrouays D, Leenaars J G B, Richer-de-Forges A C, Adhikari K, Ballabio C, Greve M, Grundy M, Guerrero E, Hempel J, Hengl T, Heuvelink G, Batjes N, Carvalho E, Hartemink A, Hewitt A, Hong S Y, Krasilnikov P, Lagacherie P, Lelyk G, Libohova Z, Lilly A, McBratney A, McKenzie N, Vasquez G M, Mulder V L, Minasny B, Montanarella L, Odeh I, Padarian J, Poggio L, Roudier P, Saby N, Savin I, Searle R, Solbovoy V, Thompson J, Smith S, Sulaeman Y, Vintila R, Rossel R V, Wilson P, Zhang G L, Swerts M, Oorts K, Karklins A, Feng L, Ibelles Navarro A R, Levin A, Laktionova T, Dell'Acqua M, Suvannang N, Ruam W, Prasad J, Patil N, Husnjak S, Pásztor L, Okx J, Hallett S, Keay C, Farewell T, Lilja H, Juilleret J, Marx S, Takata Y, Kazuyuki Y, Mansuy N, Panagos P, van Liedekerke M, Skalsky R, Sobocka J, Kobza J, Eftekhari K, Alavipanah S K, Moussadek R, Badraoui M, Da Silva M, Paterson G, da Conceição Gonçalves M, Theocharopoulos S, Yemefack M, Tedou S, Vrscaj B, Grob U, Kozák J, Boruvka L, Dobos E, Taboada M, Moretti L, Rodriguez D. 2017b. Soil legacy data rescue *via* GlobalSoilMap and other international and national initiatives. *GeoResJ.* **14**: 1–19.

Arrouays D, McBratney A, Bouma J, Libohova Z, Richer-de-Forges A C, Morgan C L S, Roudier P, Poggio L, Mulder V L. 2020. Impressions of digital soil maps: The good, the not so good, and making them ever better. *Geoderma Regional.* **20**: e00255.

Arrouays D, McKenzie N, Hempel J, Richer-de-Forges A C, McBratney A. 2014b. GlobalSoilMap: Basis of the Global Spatial Soil Information System. CRC Press, Boca Raton.

Ballabio C, Panagos P, Monatanarella L. 2016. Mapping topsoil physical properties at European scale using the LUCAS database. *Geoderma.* **261**: 110–123.

Bazaglia Filho O, Rizzo R, Lepsch I F, Prado H D, Gomes F H, Mazza J A, Demattê J A M. 2013. Comparison between detailed digital and conventional soil maps of an area with complex geology. *Rev Bras Ciênc Solo.* **37**: 1136–1148.

Biggs A J W, Crawford M, Andrews K, Sugars M, Smith D, Brown W. 2021. On the accuracy of soil survey in Queensland, Australia. *Soil Res.* **59**: 359–372.

Bishop T F A, Horta A, Karunaratne S B. 2015. Validation of digital soil maps at different spatial supports. *Geoderma.* **241-242**: 238–249.

Bivand R, Rundel C, Pebesma E, Stuetz R, Hufthammer K O, Giraudoux P, Davis M, Santilli S. 2021. rgeos: Interface to geometry engine—open source ('GEOS'). Available online at http://mirrors.ustc.edu.cn/CRAN/web/packages/rgeos/ (verified on July 18, 2023).

Brus D J, Kempen B, Heuvelink G B M. 2011. Sampling for validation of digital soil maps. *Eur J Soil Sci.* **62**: 394–407.

Carlile P, Bui E, Moran C, Minasny B, McBratney A B. 2001. Estimating Soil Particle Size Distributions and Percent Sand, Silt and Clay for Six Texture Classes Using the Australian Soil Resource Information System Point Database. CSIRO Land and Water, Canberra.

Caubet M, Román Dobarco M, Arrouays D, Minasny B, Saby N P A. 2019. Merging country, continental and global predictions of soil texture: Lessons from ensemble modelling in France. *Geoderma.* **337**. 99–110.

Chen S, Mulder V L, Heuvelink G B M, Poggio L, Caubet M, Román Dobarco M, Walter C, Arrouays D. 2020. Model averaging for mapping topsoil organic carbon in France. *Geoderma*: **366**: 114237.

Chen S, Richer-de-Forges A C, Mulder V L, Martelet G, Loiseau T, Lehmann S, Arrouays D. 2021. Digital mapping of the soil thickness of loess deposits over a calcareous bedrock in Central France. *Catena.* **198**: 105062.

Chen S, Arrouays D, Mulder V L, Poggio L, Minasny B, Roudier P, Libohova Z, Lagacherie P, Shi Z, Hannam J, Meersmans J, Richer-de-Forges A C, Walter C. 2022. Digital mapping of GlobalSoilMap soil properties at a broad scale: A review. *Geoderma.* **409**: 115567.

David O O. 1999. Improvement in field texture accuracy for sustainable agriculture. *J Sustainable Agric.* **15**: 61–68.

Dierke C, Werban U. 2013. Relationships between gamma-ray data and soil properties at an agricultural test site. *Geoderma.* **199**: 90–98.

Ellili-Bargaoui Y, Malone B P, Michot D, Minasny B, Vincent S, Walter C, Lemercier B. 2020. Comparing three approaches of spatial disaggregation of legacy soil maps based on the Disaggregation and Harmonisation of Soil Map Units Through Resampled Classification Trees (DSMART) algorithm. *Soil.* **6**: 371–388.

Ellili-Bargaoui Y, Walter C, Michot D, Saby N P A, Vincent S, Lemercier B. 2019. Validation of digital maps derived from spatial disaggregation of legacy soil maps. *Geoderma.* **356**: 113907.

Foss J E, Wright W R, Coles R H. 1975. Testing the accuracy of field textures. *Soil Sci Soc Am J.* **39**: 800–802.

Franzmeier D P, Owens P R. 2008. Soil texture estimates: A tool to compare texture-by-feel and lab data. *J Nat Resour Life Sci Educ.* **37**: 111–116.

Gray J M, Bishop T F A, Wilford J R. 2016. Lithology and soil relationships for soil modelling and mapping. *Catena.* **147**: 429–440.

Guevara M, Olmedo G F, Stell E, Yigini Y, Aguilar Duarte Y, Arellano Hernández C, Arévalo G E, Arroyo-Cruz C E, Bolivar A, Bunning S, Bustamante Cañas N, Cruz-Gaistardo C O, Davila F, Dell Acqua M, Encina A, Figueredo Tacona H, Fontes F, Hernández Herrera J A, Ibelles Navarro A R, Loayza V, Manueles A M, Mendoza Jara F, Olivera C, Osorio Hermosilla R, Pereira G, Prieto P, Alexis Ramos I, Rey Brina J C, Rivera R, Rodríguez-Rodríguez J, Roopnarine R, Rosales Ibarra A, Rosales Riveiro K A, Schulz G A, Spence A, Vasques G M, Vargas R R, Vargas R. 2018. No silver bullet for digital soil mapping: Country-specific soil organic carbon estimates across Latin America. *Soil.* **4**: 173–193.

Head J S, Crockatt M E, Didarali Z, Woodward M J, Emmett B A. 2020. The role of citizen science in meeting SDG targets around soil health. *Sustainability.* **12**: 10254.

Heitkamp F, Ahrends B, Evers J, Meesenburg H. 2021. Spatial 3D mapping of forest soil carbon stocks in Hesse, Germany. *J Plant Nutr Soil Sci.* **184**: 635–656.

Helfenstein A, Mulder V L, Heuvelink G B M, Okx J P. 2022. Tier 4 maps of soil pH at 25 m resolution for the Netherlands. *Geoderma.* **410**: 115659.

Hengl T, de Jesus J M, MacMillan R A, Batjes N H, Heuvelink G B M, Ribeiro E, Samuel-Rosa A, Kempen B, Leenaars J G B, Walsh M G, Gonzalez M R. 2014. SoilGrids1km—Global soil information based on automated mapping. *PLOS ONE.* **9**: e105992.

Heuvelink G B M, Pebesma E J. 1999. Spatial aggregation and soil process modelling. *Geoderma*. **89**: 47–65.

Hodgson J M, Hollis J M, Jones R J A, Palmer R C. 1976. A comparison of field estimates and laboratory analyses of the silt and clay contents of some west midland soils. *Eur J Soil Sci*. **27**: 411–419.

Holmes K W, Griffin E A, Odgers N P. 2015. Large-area spatial disaggregation of a mosaic of conventional soil maps: Evaluation over western Australia. *Soil Res*. **53**: 865–880.

Institut national de l'information géographique et forestière (IGN). 2011. BD ALTI® version 2.0. Le modèle numérique de terrain (MNT) maillé qui décrit le relief du territoire français à moyenne échelle (in French). Available online at https://geoservices.ign.fr/bdalti (verified on July 21, 2023).

Jamagne M. 1967. Bases et techniques d'une cartographie des sols. *Ann Agron* (in French). **18**: 1–142.

Lacoste M, Lemercier B, Walter C. 2011. Regional mapping of soil parent material by machine learning based on point data. *Geomorphology*. **133**: 90–99.

Lagacherie P, Bailly J S, Monestiez P, Gomez C. 2012. Using scattered hyperspectral imagery data to map the soil properties of a region. *Eur J Soil Sci*. **63**: 110–119.

Liu F, Zhang G L, Song X D, Li D C, Zhao Y G, Yang J L, Wu H Y, Yang F. 2020. High-resolution and three-dimensional mapping of soil texture of China. *Geoderma*. **361**: 114061.

Loiseau T, Richer-de-Forges A C, Martelet G, Bialkowski A, Nehlig P, Arrouays D. 2020. Could airborne gamma-spectrometric data replace lithological maps as co-variates for digital soil mapping of topsoil particle-size distribution? A case study in western France. *Geoderma Regional*. **22**: e00295.

Ma Y X, Minasny B, Malone B P, Mcbratney A B. 2019. Pedology and digital soil mapping (DSM). *Eur J Soil Sci*. **70**: 216–235.

Machado I R, Giasson E, Campos A R, Costa J F F, da Silva E B, Bonfatti B R. 2018. Spatial disaggregation of multi-component soil map units using legacy data and a tree-based algorithm in southern Brazil. *Rev Bras Ciênc Solo*. **42**: e0170193.

Malone B, Searle R. 2021. Updating the Australian digital soil texture mapping (Part 1*): Re-calibration of field soil texture class centroids and description of a field soil texture conversion algorithm. *Soil Res*. **59**: 419–434.

Martelet G, Drufin S, Tourliere B, Saby N P A, Perrin J, Deparis J, Prognon F, Jolivet C, Ratié C, Arrouays D. 2013. Regional regolith parameter prediction using the proxy of airborne gamma ray spectrometry. *Vadose Zone J*. **12**: 1–14.

Martelet G, Nehlig P, Arrouays D, Messner F, Tourlière B, Laroche B, Deparis J, Saby N P A, Richer-de-Forges A C, Jolivet C, Ratié C. 2014. Airborne gamma-ray spectrometry: Potential for regolith-soil mapping and characterization. *In* Arrouays D, McKenzie N, Hempel J, Richer-de-Forges A C, McBratney A (eds.) GlobalSoilMap: Basis of the Global Spatial Soil Information System. CRC Press, Boca Raton. pp. 401–408.

McBratney A B, Mendonça Santos M L, Minasny B. 2003. On digital soil mapping. *Geoderma*. **117**: 3–52.

Megumi K, Mamuro T. 1977. Concentration of uranium series nuclides in soil particles in relation to their size. *J Geophys Res*. **82**: 353–356.

Meinshausen N. 2006. Quantile regression forests. *J Mach Learn Res*. **7**: 983–999.

Minasny B, McBratney A B. 2001. The Australian soil texture boomerang: A comparison of the Australian and USDA/FAO soil particle-size classification systems. *Aust J Soil Res*. **39**: 1443–1451.

Minasny B, McBratney A B. 2016. Digital soil mapping: A brief history and some lessons. *Geoderma*. **264**: 301–311.

Moeys J, Shangguan W, Petzold R, Minasny B, Rosca B, Jelinski N, Zelazny W, Souza R M S, Safanelli J L, ten Caten A. 2018. R Package Soiltexture: Functions for soil texture plot, classification and transformation. Version 1.5.1. Available online at https://cran.r-project.org/web/packages/soiltexture/soiltexture.pdf (verified on July 21, 2023).

Møller A B, Malone B, Odgers N P, Beucher A, Iversen B V, Greve M H, Minasny B. 2019. Improved disaggregation of conventional soil maps. *Geoderma*. **341**: 148–160.

Mulder V L, Lacoste M, Richer-de-Forges A C, Arrouays D. 2016. Global-SoilMap France: High-resolution spatial modelling the soils of France up to two meter depth. *Sci Total Environ*. **573**: 1352–1369.

National Soil Survey Center, Natural Resources Conservation Service, US Department of Agriculture (NSSC-NRCS-USDA). 2012. Field Book for Describing and Sampling Soils. Version 3.0. Books Express Publishing, Lincoln.

Nauman T W, Thompson J A. 2014. Semi-automated disaggregation of conventional soil maps using knowledge driven data mining and classification trees. *Geoderma*. **213**: 385–399.

Nédélec H. 2015. Carte des sols de Pithiviers au 1/50 000 (in French). Editions Chambre d'Agriculture du Loiret, Orléans.

Odgers N P, McBratney A B, Minasny B, Sun W, Clifford D. 2014a. DSMART: An algorithm to spatially disaggregate soil map units. *In* Arrouays D, McKenzie N, Hempel J, Richer-de-Forges A C, McBratney A (eds.) GlobalSoilMap: Basis of the Global Spatial Soil Information System. CRC Press, Boca Raton. pp. 261–266.

Odgers N P, Sun W, McBratney A B, Minasny B, Clifford D. 2014b. Disaggregating and harmonising soil map units through resampled classification trees. *Geoderma*. **214-215**: 91–100.

Orgiazzi A, Ballabio C, Panagos P, Jones A, Fernández-Ugalde O. 2018. LUCAS soil, the largest expandable soil dataset for Europe: A review. *Eur J Soil Sci*. **69**: 140–153.

Padarian J, Minasny B, McBratney A B, 2019. Using deep learning for digital soil mapping. *Soil*. **5**: 79–89.

Padarian J, Minasny B, McBratney A B. 2020. Machine learning and soil sciences: A review aided by machine learning tools. *Soil*. **6**: 35–52.

Poggio L, de Sousa L M, Batjes N H, Heuvelink G B M, Kempen B, Ribeiro E, Rossiter D. 2021. SoilGrids 2.0: Producing soil information for the globe with quantified spatial uncertainty. *Soil*. **7**: 217–240.

Poggio L, Gimona A, Brewer M J. 2013. Regional scale mapping of soil properties and their uncertainty with a large number of satellite-derived covariates. *Geoderma*. **209-210**: 1–14.

Post D F, Huete A R, Pease D S. 1986. A comparison of soil scientist estimations and laboratory determinations of some Arizona soil properties. *J Soil Water Conserv*. **41**: 421–424.

Richer-de-Forges A C, Arrouays D, Bardy M, Bispo A, Lagacherie P, Laroche B, Lemercier B, Sauter J, Voltz M. 2019. Mapping of soils and land-related environmental attributes in France: Analysis of end-users' needs. *Sustainability*. **11**: 2940.

Richer-de-Forges A C, Arrouays D, Chen S, Román Dobarco M, Libohova Z, Roudier P, Minasny B, Bourennane H. 2022. Hand-feel soil texture and particle-size distribution in Central France. Relationships and implications. *Catena*. **213**: 106155.

Richer-de-Forges A C, Feller C, Jamagne M, Arrouays D D. 2008a. Perdus dans le triangle des textures. *Etude et Gestion des Sols* (in French). **15**: 97–111.

Richer-de-Forges A C, Renaux B, Verbèque B, Soucémarianadin L, Eimberck M. 2008b. Référentiel Régional Pédologique de la Région Centre: Carte des Pédopaysages du Loiret à 1/250 000 (in French). Editions QUAE, Paris.

Rossiter D G, Liu J, Carlisle S, Zhu A X. 2015. Can citizen science assist digital soil mapping? *Geoderma*. **259-260**: 71–80.

Rossiter D G, Poggio L, Beaudette D, Libohova Z. 2021. How well does Predictive Soil Mapping represent soil geography? An investigation from the USA. Case studies. International Soil Reference and Information Centre, Wageningen.

Roudier P, Burge O R, Richardson S J, McCarthy J K, Grealish G J, Ausseil A G. 2020. National scale 3D mapping of soil pH using a data augmentation approach. *Remote Sens*. **12**: 2872.

Salley S W, Herrick J E, Holmes C V, Karl J W, Levi M R, McCord S E, van der Waal C, van Zee J W. 2018. A comparison of soil texture-by-feel estimates: Implications for the citizen soil scientist. *Soil Sci Soc Am J*. **82**: 1526–1537.

Szatmári G, Pásztor L, Heuvelink G B M. 2021. Estimating soil organic carbon stock change at multiple scales using machine learning and multivariate geostatistics. *Geoderma*. **403**: 115356.

Thierion V, Vincent A, Valero S. 2022. Theia OSO Land Cover Map 2021.Version 1. Available online at https://doi.org/10.5281/zenodo.653 8910 (verified on July 21, 2023).

Tifafi M, Guenet B, Hatté C. 2018. Large differences in global and regional total soil carbon stock estimates based on SoilGrids, HWSD, and NCSCD: Intercomparison and evaluation based on field data from USA, England, Wales, and France. *Global Biogeochem Cy*. **32**: 42–56.

Ungaro F, Staffilani F, Tarocco P. 2010. Assessing and mapping topsoil organic carbon stock at regional scale: A Scorpan Kriging approach conditional on soil map delineations and land use. *Land Degrad Dev*. **21**: 565–581.

Vaysse K, Heuvelink G B M, Lagacherie P. 2017. Spatial aggregation of soil property predictions in support of local land management. *Soil Use Manage*. **33**: 299–310.

Vincent S, Lemercier B, Berthier L, Walter C. 2018. Spatial disaggregation of complex Soil Map Units at the regional scale based on soil-landscape relationships. *Geoderma*. **311**: 130–142.

Vitharana U W A, Mishra U, Mapa R B. 2019. National soil organic carbon estimates can improve global estimates. *Geoderma*. **337**: 55–64.

Voltz M, Arrouays D, Bispo A, Lagacherie P, Laroche B, Lemercier B, Richer-de-Forges A, Sauter J, Schnebelen N. 2020. Possible futures of soil-mapping in France. *Geoderma Regional*. **23**: e00334.

Vos C, Don A, Prietz R, Heidkamp A, Freibauer A. 2016. Field-based soil-texture estimates could replace laboratory analysis. *Geoderma*. **267**: 215–219.

Wilford J. 2012. A weathering intensity index for the Australian continent using airborne gamma-ray spectrometry and digital terrain analysis. *Geoderma*. **183–184**: 124–142.

Wright M N, Ziegler A. 2017. ranger: A fast implementation of random forests for high dimensional data in C++ and R. *J Stat Soft*. **77**: 1–17.

Zhang G L, Liu F, Song X D. 2017. Recent progress and future prospect of digital soil mapping: A review. *J Integr Agric*. **16**: 2871–2885.